Coupling between octahedral tilting and ferroelectric order in tetragonal tungsten bronze-structured dielectrics

Igor Levin[a)]
Ceramics Division, National Institute of Standards and Technology, Gaithersburg, Maryland 20899

Martin C. Stennett, Gabrielle C. Miles, David. I. Woodward,
Anthony R. West, and Ian M. Reaney
Department of Engineering Materials, University of Sheffield, Sir Robert Hadfield Building, Sheffield S1 3JD, United Kingdom

(Received 17 April 2006; accepted 27 July 2006; published online 20 September 2006)

Strong coupling between local polar displacements and a commensurate octahedral tilting is proposed to explain the onset of classic ferroelectric behavior in tetragonal tungsten bronzelike dielectrics $Ba_2La_xNd_{1-x}Nb_3Ti_2O_{15}$. The ferroelectric phase transition is associated with a discontinuous *non-lock-in* transformation of an incommensurate tilted structure to a commensurate superstructure. In a manner reminiscent of perovskitelike oxides, the driving force for commensurate tilting increases as the average ionic radius of the rare-earth ion decreases; no classical ferroelectric transition is observed for compositions with $x>0.75$, which remain incommensurate and exhibit only relaxor behavior below room temperature. © *2006 American Institute of Physics*. [DOI: 10.1063/1.2355434]

Complex oxides crystallizing with tetragonal tungsten bronzelike structures constitute one of the major families of dielectrics which are known to exhibit either ferroelectric or relaxor ferroelectric behavior.[1] The tetragonal tungsten bronze (TTB) structures, which can be viewed as perovskite derivatives $A_x\square_{1-x}BX_3$ with $x<0.75$,[2] consist of layers of $[BX_6]$ octahedra (Fig. 1) sharing corners to form pentagonal ($A1$), square ($A2$), and trigonal (C) tunnels, which are stacked so that the octahedra in the adjacent layers share corners.[2] The larger A cations typically reside in the pentagonal and square tunnels, although examples of compounds with smaller cations occupying the triangular tunnels are known. The ideal TTB structures exhibit a tetragonal $P4/mbm$ symmetry with $a_o\approx 12.4$ Å and $c_o\approx 4$ Å.

Recently, novel ceramics with promising ferroelectric properties for capacitor applications have been reported in the TTB-like systems $Ba_2ReTi_3Nb_2O_{15}$ (Re=rare earth).[3,4] Further studies of these materials with Re=Bi^{3+}, La^{3+}, Nd^{3+}, Sm^{3+}, and Gd^{3+} demonstrated that both Bi- and La-based compounds exhibit *relaxorlike* behavior, whereas their Nd-, Sm-, and Gd-based analogs are *classical* ferroelectrics.[5,6]

X-ray diffraction patterns of the $Ba_2ReNb_3Ti_2O_{15}$ (Re=Bi^{3+}, La^{3+}, Nd^{3+}, Sm^{3+}, and Gd^{3+}) compounds have been indexed using a prototype tetragonal TTB cell,[6] and the structure of $Ba_2LaNb_3Ti_2O_{15}$ has been refined using both x-ray and neutron powder diffractions.[5] The refinements, which confirmed segregation of Ba and La into the pentagonal and square tunnels, respectively, suggested occurrence of a $P4/mbm\rightarrow P4bm$ phase transition between 400 and 100 K, accompanied by polar displacements of Nb and Ti along the c axis. However, electron microscopy studies of the $Ba_2ReNb_3Ti_2O_{15}$ compounds[5,6] revealed deviations from the ideal TTB symmetry caused by two distinct types of two-dimensional structural modulations: (type 1) an incommensurate (IC) modulation described by the wave vectors $\mathbf{q}_1=(\frac{1}{4}+\delta)(\mathbf{a}_o^*+\mathbf{b}_o^*)$, $\mathbf{q}_2=\frac{1}{2}\mathbf{c}_o^*$ (asterisk indicates reciprocal space), which was observed for both Bi- and La-based relaxorlike compounds, and (type 2) a commensurate modulation with $\mathbf{q}_1=\frac{1}{2}(\mathbf{a}_o^*+\mathbf{b}_o^*)$, $\mathbf{q}_2=\frac{1}{2}\mathbf{c}_o^*$, as observed for the Nd-, Sm-, and Gd-based phases exhibiting classical ferroelectric behavior. The first modulation, if commensurate ($\delta=0$), would give rise to an orthorhombic supercell with $a\approx 2\sqrt{2}a_o$, $b\approx\sqrt{2}a_o$, $c\approx 2_o$. The second modulation generates an orthorhombic supercell with the lattice parameters $a\approx b\approx\sqrt{2}a_o$ and $c\approx 2c_o$.

The IC modulation (type 1) is encountered in numerous TTB ferroelectrics [e.g., $Ba_2NaNb_5O_{15}$,[7,8] $Ba_xSr_{1-x}Nb_2O_6$ (Refs. 9–11) and has been studied extensively using various diffraction and imaging techniques. Most structural studies agree that this modulation is associated with octahedral tilting;[8,11,12] however, the correct representation of its nature (i.e., intergrowth[10] versus harmonic[11,12]) remains debatable. The commensurate (type 2) modulation so far has been observed only for the $Ba_2ReNb_3Ti_2O_{15}$ (Re=Nd, Gd, and Sm) compounds[6] and no detailed structural studies of this modulation have yet been reported. The appearance of this commensurate structure has been attributed to a relatively small size[13] of the Nd, Gd, and Sm ions (<1.3 Å) as compared to La, Bi, Na, Sr, and Pb (>1.3 Å), which typically reside in the square tunnels of the TTB structures.[6] In the present contribution, we conducted a variable-temperature study of the structural behavior and dielectric properties in the $BaLaNb_3Ti_2O_{15}$–$BaNdNb_3Ti_2O_{15}$ system to determine the relation between the two types of structural modulation and their effects on the dipolar order.

The $Ba_2La_{1-x}Nd_xNb_3Ti_2O_{15}$ ceramic samples with $x=0$, $\frac{1}{4}$, $\frac{1}{2}$, $\frac{3}{4}$, and 1 were synthesized using a conventional mixed-

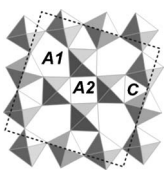

FIG. 1. Schematic diagram of the TTB structure projected along the c axis. The pentagonal ($A1$), square ($A2$), and trigonal (C) sites are indicated.

[a)]Electronic mail: igor.levin@nist.gov

 © 2006 American Institute of Physics
Downloaded 30 Mar 2007 to 129.6.122.189. Redistribution subject to AIP license or copyright, see http://apl.aip.org/apl/copyright.jsp

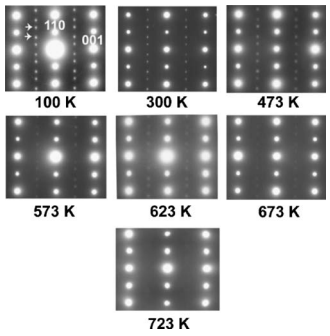

FIG. 2. Variable-temperature $[110]_o$ zone axis electron diffraction patterns recorded from a single grain of the $Ba_2LaNb_3Ti_2O_{15}$ compound. The fundamental reflections are indexed according to the ideal TTB tetragonal cell. Note the gradual disappearance of the satellite reflections at $h+(\frac{1}{4}-\delta)$, $k+(\frac{1}{4}-\delta)$, and $l+\frac{1}{2}$, which manifest an IC$\leftrightarrow P4/mbm$ transition.

oxide processing route as detailed in Ref. 6. The equilibrated single-phase powders were sintered at 1450 °C in air for 4 h on a zirconia tile. The phase purity of the samples was confirmed using x-ray powder diffraction. The samples were analyzed in transmission electron microscope (TEM) equipped with the heating/cooling sample holders and operated at 200 kV. Variable-temperature dielectric measurements were conducted in the frequency range from 5 Hz to 13 MHz using an impedance analyzer.

As reported previously,[5,6] room-temperature electron diffraction patterns of $Ba_2LaNb_3Ti_2O_{15}$ exhibit incommensurate satellite reflections $h+(\frac{1}{4}-\delta)$, $k+(\frac{1}{4}-\delta)$, $l+\frac{1}{2}$ in the $(110)_o$ (subscript o refers to the ideal $a_o\times c_o$ TTB cell) but not the $(1\bar{1}0)_o$, reciprocal lattice sections of the fundamental tetragonal structure.[6] *In situ* heating experiments for this compound revealed a reversible IC$\leftrightarrow P4/mbm$ phase transition around $T=473$ K (Fig. 2). The transition temperature was defined as the temperature at which the appearance of satellite reflections, as visually observed in the diffraction patterns, changes from sharp to diffuse; however, the diffuse satellite spots were still visible at higher temperatures before disappearing at $T>725$ K. *In situ* cooling of the IC phase down to 100 K produced neither *lock in* to a commensurate structure nor any other phase transition. The parameter δ, which describes the deviation from commensurate periodicity $(2\sqrt{a_o})$ along the $[110]_o$ direction of the basic TTB cell, varies from 0.050 to 0.034 with the temperature decreasing from 473 to 100 K, respectively. Assuming $\delta=0$, the reflection conditions in the electron diffraction patterns fit both the *Amam* and *Ama*2 symmetries ($a\approx 2\sqrt{2a_o}$, $b\approx\sqrt{2a_o}$, and $c\approx 2_o$). The *Ama*2 space group is consistent with the noncentric symmetry identified for the average $Ba_2LaNb_3Ti_2O_{15}$ structure at low temperatures.[5] This space group has been reported previously for a commensurate approximant of the IC phase in the TTB-like compounds $Ba_2NaNb_5O_{15}$,[8] $Ba_xSr_{1-x}Nb_2O_6$,[11] and $K_{0.525}FeF_3$.[12]

Room-temperature electron diffraction patterns and the reconstructed reciprocal lattice for the $Ba_2NdNb_3Ti_2O_{15}$ compound have also been reported previously.[6] The reflection conditions suggest an orthorhombic unit cell with $a\approx b\approx\sqrt{2a_o}$ and $c\approx 2c_o$ and either *Imam* or *Ima*2 symmetry; however, its room-temperature ferroelectric response suggests that the latter noncentric space group is correct. Cooling this sample down to 100 K produced no detectable changes in the *Ima*2 structure, while heating above ~400 K induced a reversible phase transition to an incommensurate

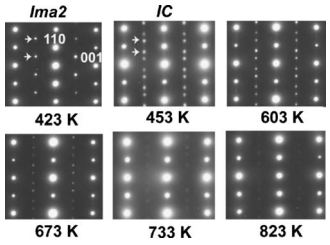

FIG. 3. Variable-temperature $[110]_o$ zone axis electron diffraction patterns recorded from a single grain of the $Ba_2NdNb_3Ti_2O_{15}$ compound. The reflections are indexed according to the ideal tetragonal TTB cell. The *Ima*2 superstructure reflections at $h+\frac{1}{2}$, $k+\frac{1}{2}$, and $l+\frac{1}{2}$ are replaced by the IC satellites at $T\approx 400$ K, which gradually disappear at higher temperatures, consistent with a sequence of phase transitions *Ima*2$\leftrightarrow$IC$\leftrightarrow P4/mbm$.

structure with satellite reflections at the positions $h+(\frac{1}{4}-\delta)$, $k+(\frac{1}{4}-\delta)$, and $l+\frac{1}{2}$ (Fig. 3). The reciprocal lattice of this high-temperature incommensurate form of $Ba_2NdNb_3Ti_2O_{15}$ was identical to that of the room-temperature form of $Ba_2LaNb_3Ti_2O_{15}$ (Fig. 2). The *Ima*2$\leftrightarrow$IC transformation was abrupt, consistent with a first-order transition. Further heating caused gradual disappearance of the incommensurate reflections, which vanished above 820 K, indicating a transition to the prototype tetragonal TTB structure (Fig. 3). Since $Ba_2NdNb_3Ti_2O_{15}$ is paraelectric above 400 K,[6] we assumed $P4/mbm$ rather than $P4bm$ symmetry for the high-temperature polymorph. The IC$\leftrightarrow$*Ima*2 transition is not of the lock-in type, since it relates two distinct structural modulations.

Similar heating/cooling analyses of the $Ba_2La_xNd_{1-x}Nb_3Ti_2O_{15}$ $(x=\frac{1}{4},\frac{1}{2},\frac{3}{4})$ samples confirmed the occurrence of a phase transition sequence *Ima*2$\leftrightarrow$IC$\leftrightarrow P4/mbm$ across the solid solutions with the transition temperatures decreasing with the increasing La content. The samples typically exhibited a grain-to-grain variation of the transition temperature with the broadest range observed for the $x=\frac{1}{2}$ composition, where a mixture of the IC and *Ima*2 phases was present down to 100 K. The $x=\frac{3}{4}$ sample also contained a residual IC phase at low temperatures. The *Ima*2$\leftrightarrow$IC transition temperature, as determined using electron diffraction, decreases from $\approx$350 K for $x=0.25$ to $\approx$265 K for $x=0.75$.

The results of variable-temperature dielectric measurements for the $Ba_2La_xNd_{1-x}Nb_3Ti_2O_{15}$ solid solutions are summarized in Fig. 4. The samples with $x=0$, $\frac{1}{4}$, and $\frac{3}{4}$ all exhibit a relatively sharp, frequency independent maximum of dielectric constant ε_r at the temperatures corresponding approximately to those of the IC$\leftrightarrow$*Ima*2 transition. A significantly broader maximum for the $x=\frac{1}{2}$ sample (compared to $x=0$, $\frac{1}{4}$, $\frac{3}{4}$) was attributed to a heterogeneous mixture of La and Nd causing a spread of the IC$\leftrightarrow$*Ima*2 transition temperatures, as confirmed by TEM. All four samples exhibited some frequency dispersion of the dielectric constant and di-

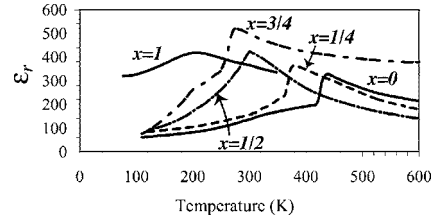

FIG. 4. Variable-temperature dielectric constant ε_r (at 1 MHz) for the solid solutions $Ba_2La_xNd_{1-x}Nb_3Ti_2O_3$.

Downloaded 30 Mar 2007 to 129.6.122.189. Redistribution subject to AIP license or copyright, see http://apl.aip.org/apl/copyright.jsp

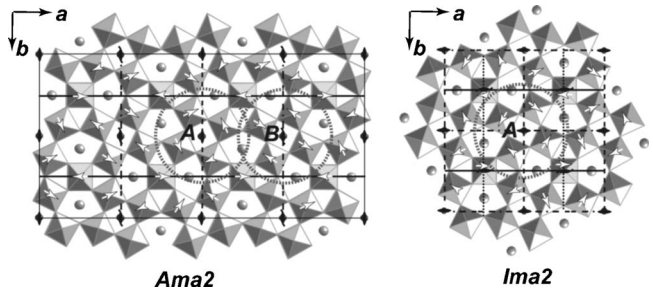

FIG. 5. Schematic diagram describing the octahedral tilting in the *Ama*2 (left) and *Ima*2 (right) superstructures; the tilting directions are indicated using arrows. The tilting in the *Ama*2 structure, which can be predicted from symmetry considerations for an array of rigid $[BO_6]$ octahedra, has been reported in Refs. 8 and 12. The tilting in the *Ima*2 phase was obtained from the neutron powder diffraction refinements for the $Ba_2NdNb_3Ti_2O_{15}$. The diagram shows a single $(001)_o$ layer of octahedra.

electric loss at temperatures (≈200 K) below a ferroelectric phase transition; this dispersion became more pronounced with the increasing La content. For the $Ba_2LaNb_3Ti_2O_{15}$ ($x=1$), a single broad peak with a frequency dependent[6] maximum which signifies a relaxorlike behavior was observed. Thus, the TEM and dielectric measurements combined indicate that the IC↔*Ima*2 phase transition induces a long-range dipolar order yielding a classical ferroelectric transition.

As a part of the present study, we determined the nature of the displacive modulation in the *Ima*2 phase of $Ba_2NdNb_3Ti_2O_{15}$ from structural refinements using neutron powder diffraction data (for $Ba_2NdNb_3Ti_2O_{15}$, attempts to fit the *P*4/*mbm* and *P*4*bm* models to the neutron diffraction data yielded poor statistical parameters. In contrast, the *Ima*2 model provided a satisfactory fit to the experimental data). The refinement details will be reported separately. Our results confirmed that, similar to the IC structure, the *Ima*2 modulation originates from octahedral tilting (Fig. 5); however, the tilting topologies in the two structures are different. The *Ima*2 structure features a single tilting pattern [designated as A and circled in Fig. 5(b)] along with antiphase rotations of octahedra in successive layers along the *c* axis. In contrast, the *Ama*2 approximant of the IC phase exhibits two distinct tilting configurations [A and B in Fig. 5(a)] and no antiphase tilting about the *c* axis.[13]

The onset of the IC↔*Ima*2 transition in the solid solutions correlates with the size of the cations in the square tunnels, as suggested by the transition temperature, which decreases with increasing the substitution of larger La ($R=1.36$ Å)[14] for smaller Nd ($R=1.27$ Å). In the TTB structures, octahedral tilting affects the coordination environments of the cation sites in all three types of tunnels. Therefore, the type of tilting and the periodicity of the tilting modulation (commensurate or IC) are likely determined by the competing bonding requirements of the cations in the pentagonal (Ba) and square (La or Nd) tunnels. Considering the relatively small difference between the sizes of La and Nd ($\Delta R=0.09$ Å), the energy balance for the two structures must be rather subtle, and even small spatial fluctuations of the La/Nd ratio are likely to cause substantial variations of the local transition temperatures, as was observed for the solid solution samples.

The relaxor behavior observed in the La-based compound can be attributed to the occurrence of polar clusters, associated with the off-center Nb/Ti displacements, which grow in size with decreasing temperature. These polar displacements are supported by the neutron diffraction refinements at 100 K (e.g., below T_m),[5] where the clusters become large enough to produce a detectable effect on the average structure. Long-range dipolar correlations are likely precluded by the random fields associated with the chemical disorder of Ti^{4+} and Nb^{5+} cations.[15] The IC tilting modulation has been observed previously in TTB-like compounds which exhibit both relaxorlike[15] and classical ferroelectric[16] behavior, suggesting that this modulation *per se* has little effect on the dipolar order. Recent refinements of the IC modulation in $Ba_xSr_{1-x}Nb_2O_6$ compound[12] also confirmed only a weak effect of this modulation on the Nb displacements. In contrast, according to our present results, the tilting modulation in the *Ima*2 structure, being accompanied by a significant distortion of octahedra, couples strongly to the polar cation displacements so that the change in tilting type upon the IC→*Ima*2 transition promotes long-range ferroelectric ordering with a sharp maximum of dielectric constant. The residual low-temperature relaxation observed in pure $BaNdNb_3Ti_2O_{15}$ can be attributed to the remaining random-field effects, whereas for the solid solution samples, this relaxation likely originates from the residual IC phase.

The coupling of octahedral rotations to dielectric polarization has been demonstrated in other ferroelectric oxides such as $Pb(Zr,Ti)O_3$ (Ref. 17) and various Aurivillius compounds.[18] In particular, for Aurivillius phases, a ferroelectric Curie temperature scales with the tolerance factor *t* in the perovskite blocks, and the amplitude of tilting at room temperature correlates directly with the magnitude of the spontaneous polarization.[18] We believe that no such correlations between octahedral tilting and dipolar order have been reported to date for TTB-type compounds because a tilting transition of the IC↔*Ima*2 type has never previously been reported.

[1] M. E. Lines and A. M. Glass, *Principle and Applications of Ferroelectrics and Related Materials* (Oxford University Press, Oxford, 1977).
[2] R. H. Mitchell, *Perovskites: Modern and Ancient* (Almaz, Thunder Bay, ON, 2002).
[3] X. H. Zheng and X. M. Chen, J. Mater. Res. **17**, 1664 (2002).
[4] X. H. Zheng and X. M. Chen, Solid State Commun. **125**, 449 (2003).
[5] G. C. Miles, M. C. Stennett, I. M. Reaney, and A. R. West, J. Mater. Chem. **15**, 798 (2005).
[6] M. C. Stennett, I. M. Reaney, I. Levin, G. Miles, D. I. Woodward, C. Kirk, and A. R. West, J. Appl. Phys. (in press).
[7] P. B. Jamieson, S. C. Abrahams, and J. L. Bernstein, J. Chem. Phys. **50**, 4352 (1969).
[8] P. Labbe, H. Leligny, B. Raveau, J. Scheck, and J. C. Toledano, J. Phys. C **2**, 25 (1986).
[9] J. C. Toledano and J. Schneck, Solid State Commun. **16**, 1101 (1975).
[10] P. B. Jamieson, S. C. Abrahams, and J. L. Bernstein, J. Chem. Phys. **48**, 5048 (1968).
[11] A. Bursill and P. J. Lin, Acta Crystallogr., Sect. B: Struct. Sci. **B43**, 49 (1987).
[12] Th. Woike, V. Petricek, M. Dusek, N. K. Hansen, P. Fertey, C. Lecomte, A. Arakcheeva, G. Chapuis, M. Imlau, and R. Pankrath, Acta Crystallogr., Sect. B: Struct. Sci. **B59**, 28 (2002).
[13] S. Fabbrici, E. Montanari, L. Righi, G. Calestani, and A. Migliori, Chem. Mater. **16**, 3007 (2004).
[14] R. D. Shannon, Acta Crystallogr., Sect. A: Cryst. Phys., Diffr., Theor. Gen. Crystallogr. **A32**, 751 (1976).
[15] P. Lehnen, W. Kleemann, Th. Woike, and P. Pankrath, Phys. Rev. B **64**, 224109 (2001).
[16] C. A. Randall, R. Guo, A. S. Bhalla, and L. E. Cross, J. Mater. Res. **6**, 1720 (1991).
[17] C. A. Randall, M. G. Matsko, W. Cao, and A. S. Bhalla, Solid State Commun. **85**, 193 (1993).
[18] D. Y. Suarez, I. M. Reaney, and W. E. Lee, J. Mater. Res. **16**, 3140 (2001).

Downloaded 30 Mar 2007 to 129.6.122.189. Redistribution subject to AIP license or copyright, see http://apl.aip.org/apl/copyright.jsp